Journal of Analytical and Applied Pyrolysis 113 (2015) 444–453

Contents lists available at ScienceDirect

Journal of Analytical and Applied Pyrolysis

journal homepage: www.elsevier.com/locate/jaap

A new approach for bio-oil characterization based on gel permeation chromatography preparative fractionation

M. Castellví Barnés[a], J.-P. Lange[a,b,*], G. van Rossum[a,b], S.R.A. Kersten[a]

[a] University of Twente, Sustainable Process Technology; P.O. Box 217, 7500AE Enschede, The Netherlands
[b] Shell Global Solutions Int. B.V., Shell Technology Centre; P.O. Box 38000, 1030BN Amsterdam, The Netherlands

ARTICLE INFO

Article history:
Received 28 January 2015
Received in revised form 10 March 2015
Accepted 12 March 2015
Available online 13 March 2015

Keywords:
Liquefaction
Pyrolysis
Gel Permeation Chromatography
Bio-oil
FTIR
NMR

ABSTRACT

Analyzes of bio-oils obtained by direct liquefaction are obstructed by the interferences of the liquefaction solvent. We therefore developed a new analytical approach based on a preparative gel permeation chromatography (GPC) fractionation to remove the solvent from the bio-oil and, if convenient, separate the resulting bio-oil into several fractions according to molecular size. The bio-oils investigated were prepared by liquefaction of pine wood using guaiacol and a guaiacol/water mixture as reaction media. These bio-oils were fractionated and then analyzed by several techniques such as ^{13}C and ^{1}H NMR, FTIR, C:H:O analysis and carbon residue. The results were compared with those of bio-oils produced via hydrothermal liquefaction (liquefaction in water) and fast pyrolysis. The analyzes showed great differences in product distribution, composition and properties of the bio-oil. For instance, the liquefaction oils appeared to be leaner in sugar-like components and richer in aromatic molecules than pyrolysis oil. Moreover, the aromatic content in the liquefaction oils indicated that carbohydrates react to form these type of compounds. In comparison with pyrolysis, liquefaction yielded bio-oils leaner in oxygen, but with higher content of heavies (compounds with apparent molecular weight > 1000 Da). The higher concentration of heavy products resulted in liquefaction oils with higher coking tendency than pyrolysis oil. A ranking of the severity of the reaction conditions for the liquefaction experiments is proposed: Guaiacol < Guaiacol/water < Water.

1. Introduction

The increase in energy demand [1] and the environmental concern have motivated the research and development of alternatives to fossil fuels. Among these alternatives, bio-fuels stand as a clear candidate to substitute a fraction of the fossil transportation fuels, since they can be used in the existing infrastructures and can even be blended with fossil fuels. Several processes can be used to convert biomass into bio-oils, such as liquefaction or pyrolysis. However, these bio-oils are not suitable for their direct introduction into the transportation infrastructure, and require a prior upgrading, e.g. using existing refinery technologies. Here, characterization becomes crucial, since a good knowledge of the composition and structure of the bio-oils is essential for assessing the potential of bio-oils for upgrading and for selecting appropriate upgrading technologies.

Bio-oils are complex mixtures of organic compounds that cover a wide range of molecular weight, chemical functionalities and properties, thus, making their characterization a challenging process. Furthermore, when the liquefaction is performed in an organic solvent, this solvent needs to be separated from the bio-oil before characterization to avoid its interferences during the analyzes. In the liquefaction experiments presented below, guaiacol is used as reaction media because of its efficiency as a liquefaction solvent [2].

The most common fractionation technique used with bio-oils is solvent extraction. In this procedure, the affinity of the oil components for the different phases is the driving force for the fractionation. Thus, the extraction is dictated by the interplay between molecular weight and chemical functionalities, which results in ill-defined fractions. Moreover, multiple steps are involved, which makes the process time consuming, labor intensive and leads to poor mass balance closures due to the loss of analytes. Finally, the similarities in chemical structure between guaiacol and a significant fraction of the bio-oils make solvent fractionation unsuitable for the isolation of these oils.

Another common technique, distillation, requires high vacuum and relatively high temperatures because of the high boiling point of guaiacol. Performed tests led to insufficient separation of solvent

* Corresponding author at: Shell Global Solutions Int. B.V., Shell Technology Centre
Postal address: P.O. Box 38000, 1030 BN Amsterdam, The Netherlands.
Tel.: +31 206303428.
E-mail address: jean-paul.lange@shell.com (J.-P. Lange).

http://dx.doi.org/10.1016/j.jaap.2015.03.005
0165-2370/

from the bio-oil and poor mass balances. Furthermore, the use of high temperatures can cause thermal degradation of the oils [3,4].

Another fractionation technique was therefore needed, which was capable to isolate the bio-oil without altering its composition. GPC fractionation allows a clean separation of the solvent from the bio-oil based on their differences in molecular size. After isolation, the bio-oil can be characterized and compared with other oils. In addition, the resulting bio-oil can be separated into several fractions of different molecular size, which can be analyzed separately. Although GPC has been extensively used for bio-oil characterization [5–8], it has been scarcely utilized for its fractionation. Sheu et al. used GPC fractionation to separate pyrolytic tar and its hydrogenated products into fractions with different functionalities [9]. They separated heavy non-volatiles, light non-volatiles + alkanes, phenols and aromatics based on the assumption that similar chemical species have similar molecular size. Subsequently, high-resolution gas chromatography/mass spectrometry allowed them to monitor the changes in pyrolytic tar composition during hydrogenation. Andersson et al. used GPC fractionation at analytical scale to separate phenols from the high molecular weight polyaromatics in pyrolysis oils [10]. After fractionation, they analyzed the phenolic fraction by multidimensional liquid chromatography (LC–LC). They proved that the GPC and LC–LC system gives reproducible results that are comparable to reference methods. GPC fractionation has also been successfully applied at preparative scale to study the change in composition of coal extracts and solvent refined coal fractions as function of their molecular size [11–13].

The aim of this paper is to establish a fractionation and characterization procedure that allows the isolation and characterization of bio-oil, especially those obtained after direct liquefaction in organic solvents. Bio-oils submitted to the new procedure were prepared by liquefaction of pinewood in guaiacol and in a guaiacol/water (1/1 in weight) mixture at 300 °C (hereafter, GL stands for liquefaction in guaiacol, and GWL stands for liquefaction in the guaiacol/water mixture). They were then fractionated and analyzed by means of various methods such as ^{13}C and ^{1}H NMR, FTIR, C:H:O analysis and carbon residue (MCRT). The results were compared with those of fast pyrolysis oil, hydrothermal liquefaction (liquefaction in water, named WL) oil and organosolv lignin. Fractionation was performed both for oil isolation (removal of the liquefaction solvent) and for bio-oil separation into fractions of different molecular sizes.

2. Material and methods

2.1. Materials and reagents

Pine wood was purchased from Rettenmaier & Söhne GmbH (Germany). It was grinded and sieved to a particle size below 0.5 mm and afterwards dried at 105 °C during 24 h. The composition of the wood is shown in Table 1.

Guaiacol and tetrahydrofuran (THF) were purchased in Sigma–Aldrich with a purity of ≥98% and 99.9% respectively. Deuterated acetone used in ^{1}H NMR analyzes was obtained from VWR with a 99.8% purity. Deuterated methyl sulfoxyde for ^{13}C NMR was obtained from Acros Organics with a 99.8% of deuterium atom and a 0.03% of TMS. The relaxation agent used in ^{13}C NMR was Chromium (III) acetylacetonate from Sigma–Aldrich and had a purity of 99.99%.

Organosolv lignin was prepared from the same pine wood used in the experiments following the method described by Huijgen et al. [14]. Approximately 300 g of wood were treated at 200 °C during 60 min in 2.5 kg of an ethanol:water mixture (60:40 wt%). The liquid product was slowly added onto cold water to precipitate the lignin, which was then filtered, washed and dried.

Table 1
Pine wood composition.

Composition	Value	Composition	Value
Chemical analysis	wt%, dry	Ultimate analysis	wt%, dry
Cellulose	35	C	46.58
Hemicellulose	29	H	6.34
Lignin	28	O (by difference)	46.98
Alkali metals	mg/kg, dry	N	0.04
K	34	S	0.06
Mg	134		
Ca	768		
Total ash	2600		

2.2. Liquefaction

Liquefaction experiments were performed according to the procedure described in [2] and [15]. Pine wood and liquefaction solvent were introduced in a 45 ml autoclave which was then closed and rapidly heated to 300 °C in a fluidized sand bed. An initial heating rate of approximately 60 °C/min allowed to reach 90% of the reaction temperature (270 °C) within the first 4 min and reach the targeted 300 °C some 5 min later. After 30 min, the autoclave was submerged in a cool water bath to quench the reaction. Once the reactor was at room temperature, liquefaction products were recovered and analyzed for mass balance closure and characterization. First, gas was released, and the free gas volume at atmospheric pressure was measured. A sample was taken for GC analysis. Afterwards, the autoclave was opened and a slurry was filtered to provide a liquid product and a solid filter cake. The reactor was then rinsed with acetone and the wash liquor was filtered over the filter cake. The filter cake was dried at 105 °C before quantification and analysis. The filtered wash liquor was freed from acetone with a rotary evaporator (35 °C and 100 mbar) to provide a tar phase. Both liquid product and tar were combined (mixture referred to as oil) and quantified gravimetrically prior to analysis. The total amount of product (solid, tar, liquid and gas) typically amounted to more than 90 w% of the total intake (biomass and solvent).

2.3. Fast pyrolysis

The fast pyrolysis oil was obtained at 500 °C using the setup and the procedure described in [16].

Pyrolysis oil was produced in a continuous fluidized bed reactor that used sand as fluidized bed particles. The vapors formed were directed to a condenser system composed by two counter-current spray condensers and an intensive cooler placed in series. The non-condensable gases were collected and analyzed for mass balance closure. The char produced was calculated by subtracting the initial amount of sand to the total solid residue. To obtain the fast pyrolysis oil the condensates were mixed.

2.4. Fractionation

The fractionation of the oils was performed with the GPC system described in Section 2.6.1 introducing various changes. A multidraw kit was inserted to increase the injection capacity to 1.5 ml. The three analytical columns were replaced by a pre-column (PLgel 25 × 25 mm) and a column (PLgel 300 × 25 mm with 5 μm, 500 A) placed in series. Samples were dissolved in THF when necessary (to decrease their viscosity) and then filtered through a 0.45 μm syringe filter. The fractionation was performed during 50 min at room temperature and fractions were collected automatically with a fraction collector. The THF of these obtained fractions was evaporated under vacuum (10–20 mbar) and at 35 °C to obtain the

isolated bio-oil fractions. Further details about GPC Preparative Fractionation can be found in Appendix A (supporting information).

2.5. Product definition and calculation

For both liquefaction and pyrolysis experiments, gas refers to all the non-condensable gases, oil refers to the acetone soluble compounds and solid residue includes all the acetone insoluble compounds. All the yields presented in this paper are expressed in carbon percentage (C%) and are calculated using the following equations:

$$\text{Gas yield} = \frac{(\text{mole of carbon in gas} \times 12)}{(\text{gram of wood input} \times \text{carbon content of wood})} \times 100$$

$$\text{Solid yield} = \frac{(\text{gram of solid} \times \text{carbon content of solid})}{(\text{gram of wood input} \times \text{carbon content of wood})} \times 100$$

$$\text{Oil yield} = \frac{(\text{gram of oil} \times \text{carbon content of oil})}{\text{gram of wood} \times \text{carbon content of wood}} \times 100;$$

for the pyrolysis experiment.

Oil yield=100 − Gas yield − Solid yield;

for the liquefaction experiments.

$$\text{yield of aromatics in oil} = \text{aromatic content in oil} \times \text{oil yield (C\%)}$$

$$\text{Aromatics available in the lignin} = \left[\frac{\text{lignin content of wood (on weight basis)} \times \text{carbon content of lignin} \times \text{aromatic content of lignin (on carbon basis)}}{\text{carbon content of wood}}\right] \times 100$$

To calculate the gas yield, the volume percentages measured with Micro-GC (Section 2.6.6) were converted into mole percentages using the ideal gas law. Once the number of moles of each gas component was known, the total grams of carbon in the gas could be easily calculated. Carbon percentage of the oils and solids from liquefaction experiments, lignin and wood was directly analyzed with the EA. Unfortunately, no EA could be performed for the solid residue of the pyrolysis experiment since it was mixed with the sand used in the fluidized bed. Therefore, the elemental composition used to calculate the solid C% for pyrolysis oil was found in literature and corresponds to the char produced during pyrolysis of pine shave at 500 °C [17]. The aromatic content of the oil and lignin was calculated with quantitative ^{13}C NMR.

Vacuum Residue (VR) is defined as all the components in the oil with a Mw_{GPC} higher than 1000 Da. The percentage of VR is calculated using the GPC chromatogram of the studied oil. The RID signal is plotted versus the elution time and the area corresponding to the VR residue fraction is divided by the total area.

Vacuum Residue = RID area corresponding to apparent Mw > 1000 Da/Total RID area (THF decomposition peak included)

The effective H/C ratio H/C_{eff} is calculated using the following equation:

$$\frac{H}{C_{eff}} = \frac{(\text{mole H} - 2 \times \text{mole O})}{\text{mole C}}$$

The higher heating value (HHV) is calculated using the Reed's formula [18]:

$$\text{HHV} = 0.341 \times \text{carbon percentage} + 1.322 \times \text{hydrogen percentage} - 0.12 \times \text{oxygen percentage} \left(\text{MJ/kg}\right)$$

2.6. Characterization techniques

2.6.1. GPC

Molecular weight distribution of the liquefaction products was studied with Gel Permeation chromatography (GPC) using a system from Agilent Technologies 1200. Samples were dissolved in THF and then filtered through a 0.45 μm syringe filter. For the measurement, 20 μl of sample were injected to a system composed by three columns placed in series (7.5 × 300 mm, particle size 3 μm) and two detectors, a refractive index-detector (RID) and an Variable wavelength detector (VWD) operated at 254 nm. A highly crosslinked polystyrene–divinylbenzene copolymer gel was used as column packing (Varian, PLgelMIXED-bed E). The chromatography was performed during 40 min at 40 °C and with 1 ml/min of THF as eluent. The calibration to correlate elution time and molecular weight was performed using polystyrene of 162–29,510 g/mol as standard.

2.6.2. FTIR

Qualitative FTIR analyzes were performed with a Fourier Transform Infrared Spectrophotometer from Bruker using the Attenuated total reflection technique (ATR) and a deuterated triglycine sulfate detector (DTGS). 16 scans were collected per sample at a spectral resolution of 4 cm^{-1}. Absorbance was measured from 650 to 4000 cm^{-1}. Afterwards, the baseline was corrected and the spectra normalized.

2.6.3. ^{13}C NMR

For quantitative ^{13}C NMR measurements, approximately 0.25 g of bio-oil were dissolved in 0.7 ml of deuterated DMSO with a concentration of 0.1 M of $Cr(AcAc)_3$ as relaxation agent. The measurements were performed with a Bruker 600 MHz-Avance II NMR spectrometer at 40 °C, using the DMSO-d6 as internal reference. The method utilized was inverse gate decoupling with 5 s of relaxation time and 15,000 scans. Manual integration of the spectra was performed with MestReNova LITE software (version 5.2.5–5780) and according to the ^{13}C NMR regions defined below. When present, solvent peaks (DMSO, acetone or THF) were manually integrated and subtracted from the corresponding region. Since analyzes were quantitative, all carbon types had the same response factor and, therefore, carbon percentages (in mass) could be directly obtained from the area percentage of each region.

The assignment of the peaks for ^{13}C NMR was based on the papers from Ben et al. and Ingram et al. [5,19]. The range 1–54 ppm was therefore assigned to alkanes. According to these publications, both ketal and aromatic carbons can be found in the region 100–110 ppm. However, Ben et al. [5] observed only a very small percentage of aromatic carbon below 105 ppm. Accordingly, the region 54–105 ppm was assigned to aliphatic carbon with oxygenated substituents, and the region 105–166 ppm to aromatic carbon. Finally, carboxyl and carbonyl carbon could be found between 166 and 210 ppm. Alkane-like carbon was divided into carbon at the end of the alkane chain (1–25 ppm) and carbon in the middle of the alkane chain (25–54 ppm). Aliphatic carbon with an alcohol or ether substituent was found between 54 and 84 ppm, while ketal O—C—O bonds were found from 84 to 105 ppm. Aromatic carbon was separated according to their substituents: 105–166 ppm for hydrogen, 125–142 ppm for carbon, and 142–166 ppm for oxygenated substituents. Finally, carboxylic carbon was found in the 166–180 ppm region, and carbonylic carbon in the 180–210 ppm region.

2.6.4. ^{1}H NMR

For ^{1}H NMR measurements, a sample of approximately 0.1 g was dissolved in 0.7 ml of deuterated acetone. The analyzes were performed with a Bruker 400 MHz-Ascend NMR spectrometer. A relaxation time of 2 s and 128 scans were used. Integration of the spectra was performed using the same procedure described for ^{13}C NMR.

The assignation of the peaks for ^{1}H NMR was based on the papers from Ingram et al. and Mullen et al. [19,20]. Thus, the 0.5–3.0 ppm region was assigned to alkane-like hydrogen, region 3.0–5.6 ppm to aliphatic hydrogen attached to a carbon with oxygen substituents, region 5.6–9.0 ppm to aromatic hydrogen between, and region 9.0–12.0 ppm to hydrogen from aldehyde groups. Within the alkane-like hydrogen, hydrogen at least 4 bonds far from an unsaturation or heteroatom (0.5–1.5 ppm) and hydrogen 3 bonds far to an unsaturation or heteroatom (1.5–3.0 ppm) could be distinguished. The aliphatic hydrogen 2 bonds far from an heteroatom was divided into hydrogen close to an alcohol, an ether or in methylenedibenzene (3.0–5.0 ppm), and in hydrogen from a ketal group (5.0–5.6 ppm). When visible, the broad band corresponding to the hydrogen in alcohol groups appears under 3 ppm (region of the Aliphatic α to an unsaturation or an heteroatom).

2.6.5. EA and MCRT

The elemental composition of solid and liquid products was determined with an Elemental Analyser Inter Science Flash 2000. Nitrogen, carbon and hydrogen content was directly determined and oxygen percentage was calculated by difference.

The carbon residue was measured with a Micro Carbon Residue tester ACR-M3 Zematra.

2.6.6. Gas analysis

The composition of the gas formed during liquefaction was analyzed with a Micro-Gas Chromatograph (Variant CP-4900). The Micro-GC used helium as a carrier gas and contained two columns (Molsieve 5 A (10 m) and PPQ (10 m)). In the first column H_2, O_2, N_2, CH_4 and CO were analyzed while in the second column CO_2, C_2H_4, C_2H_6, C_3H_6 and C_3H_8 were detected.

2.6.7. GC–MS

GC–MS analyzes were performed with a gas chromatograph equipped with a mass spectrometer (GC 7890 A MS 5975 C, Agilent Technologies). A 5% of oil was dissolved in 95% acetone and then filtered through a 0.2 μm Whatman filter. 1 μL of sample was injected into the injector port set at 250 °C and with a split ratio of 20:1. The capillary column (Varian CP9154, 60 m, 0.25 mm, packed with 0.25 μm of 14% cyanopropyl and phenyl, 86% PDMS) was operated at a constant Helium flow of 2 ml/min during 106 min. Oven temperature was set at 45 °C during 4 min, then increased 3 °C/min and finally maintained at 280 °C during 20 min. Mass spectrometer was operated under electron ionization mode (70 eV), with a frequency of 1 scan/s, and detected a m/z range between 15 and 500. A spectral library (NIST Mass Spectral Library Version 08) was used to identify the detected compounds.

3. Results

3.1. Procedure

Four bio-oils were prepared, analyzed and compared. Three of them were obtained by liquefaction of pine wood in a 45 ml batch autoclave at 300 °C and autogenous pressure during 30 min. For each of them, a different liquefaction medium was used, namely guaiacol, a guaiacol/water mixture (weight ratio 1/1) and water (which correspond to the well-studied hydrothermal liquefaction, WL). The fourth bio-oil was obtained by fast pyrolysis at the optimal temperature and time for oil production, namely 500 °C with residence times of 20–25 min for the solid particles and below 2 seconds for the oil. Gas and solid yields were directly measured and yield of oil dissolved in the liquefaction solvent was defined as the balance. All yields were defined on carbon-basis. Vacuum Residue (VR, oil components with an $Mw_{GPC} > 1000$ Da) was estimated using the GPC chromatograms. Detailed information about preparation and analysis of the samples can be found in Section 2 (materials and methods).

The liquefaction and pyrolysis oils were fractionated into three different fractions based on molecular weight. The two heavier fractions (named middle and heavy fraction) contained bio-oil. The lightest fraction (named light fraction) consisted mainly of guaiacol for both GL and GWL, and, therefore, was not analyzed. The lightest fraction of the WL and pyrolysis oils contained the light bio-oil components and was thus analyzed. Care was taken to collect samples that were large enough (at least 0.3 g) to allow for detailed analysis (GPC, ^{13}C NMR, ^{1}H NMR and C:H:O analysis (EA)). The characterization results of the two or three fractions were numerically combined to obtain the composition of the whole bio-oil. In addition, each bio-oil was fractionated in only two fractions, one containing mainly the solvent and another containing bio-oil, to subject the bio-oil fraction to MCRT analysis.

3.2. Product yields and distribution

The presence and nature of the solvent during thermal treatment proved to have a large effect on products distribution and properties. For instance, GL, GWL and WL resulted in higher oil yields than fast pyrolysis, even though a higher temperature was used for the latter one (Fig. 1). Major differences were also observed in the yield (0–27 C%) and nature of solid residue, being unconverted wood and/or char as revealed by FTIR (Fig. C.2 in Supporting information). Finally, liquefaction led to lower gas yield than pyrolysis, probably due to a lower reaction temperature.

The differences in oil yield are most probably caused by the use of different reaction media in the four experiments. During pyrolysis, the formation of liquid intermediates inside the solid particles promote dehydration and cross-linking reactions of the components that are too heavy to vaporize during the reaction conditions. This can lead to repolymerization and, therefore, to char formation [21,22]. In contrast, the light and heavy molecules formed during the liquefaction dissolve in the solvent, which reduces the interactions between them and, presumably, reduces their subsequent repolymerization [23]. Within the three liquefaction experiments,

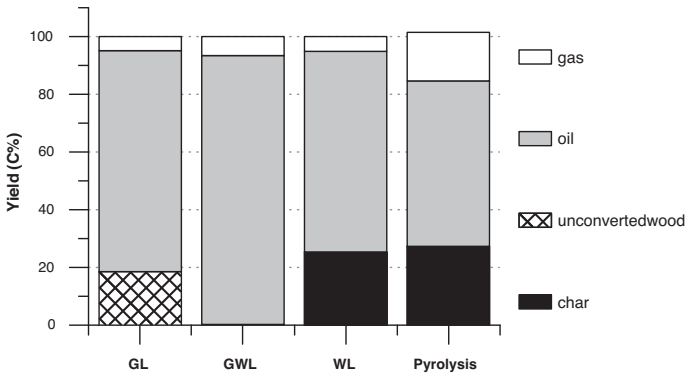

Fig. 1. Product distribution for liquefaction and pyrolysis experiments. Liquefaction experiments performed at 300 °C during 30 min with 10 wt% of wood and 90 wt% of solvent (guaiacol, guaiacol/water and water). Pyrolysis experiment performed at 500 °C with residence times of 20–25 min for the solid particles and below 2 s for the oil.

which were already reported in a previous publication [2], GWL lead to the highest liquid yields, with more than 90C% of the biomass input being converted to oil. It should be noted that, since the oil yield is calculated by difference, it includes the organics dissolved both in the organic and in the aqueous phase that was present in GWL and WL. However, GC–MS analysis of these aqueous phases revealed minor amounts of light oxygenates such as acetic acid and guaiacol. Hence, no further analysis was undertaken as the main research focuses on the analysis of the middle and heavy fractions of the bio-oils.

GL lead to a high solid yield (19 C%, Fig. 1). However, this solid consisted mainly of unconverted cellulose, as indicated by the carbohydrate fingerprint shown in its FTIR (Fig. C.2 in Supporting information) and its atomic composition represented in Fig. 6. Cellulose is the most recalcitrant component of the wood [24] and, therefore, the last component to decompose. Compared to the GL, GWL led to a remarkably low solid yield (0.3 C%, Fig. 1) that contained both unconverted carbohydrates and aromatic components (Fig. C.2 in Supporting information). Finally, a high solid yield was obtained with WL (25C%). The WL solid however, resembled the liquefaction oil and consisted on oxygenated aromatic char (Fig. C.2 in Supporting information). These results are in agreement with the data reported by Kumar et al. [15], who observed a change in the composition of the solid residue from wood-type to lignin- type to oxygenated char when the process severity (namely reaction temperature) was increased.

The three liquefaction experiments had a similar gas yield of 5–7C% whereas pyrolysis experiment led to a higher gas production of 17 C% (Fig. 1). These results are likely due to difference in reaction temperatures, i.e. 300 °C for the liquefaction and 500 °C for pyrolysis. Indeed, Kumar et al. [15] also observed an increase in gas yield with increasing reaction temperature. However, Knezevic et al. [25] observed no variation in the gas yields upon varying the reaction medium at constant temperature, i.e. with the presence (WL) or absence (pyrolysis) of water.

Based on the product distribution and the composition of the solid, a ranking of the severity of the reaction conditions can be proposed: GL < GWL < WL. Pyrolysis cannot be clearly placed in the ranking since the solid is maintained in the reactor for longer residence times than the oil, which rapidly leaves the reactor as vapor and cools down in the condensers.

3.3. Characterization of the whole bio-oil

For the characterization of the whole bio-oil without the liquefaction solvent, the results of the two or three bio-oil fractions were numerically combined to obtain the overall oil composition (for more details, see Section 3.1). In addition, each bio-oil was fractionated into only two fractions, one containing mainly the solvent and another containing bio-oil. The bio-oil fraction was subjected to MCRT analysis.

3.3.1. GPC and MCRT analyzes

The apparent molecular weight distribution (Mw_{GPC}) of the bio-oils shows significantly less heavy molecules for pyrolysis oil (up to 2000 Da) than the liquefaction oils (up to 5000 Da for WL and GWL or up to 9000 Da for GL) (Fig. 2). These results are in agreement with data found in literature [25]. Thus, liquefaction oils have a higher concentration of Vacuum Residue (VR, compounds with an Mw_{GPC} higher than 1000 Da) than pyrolysis oil.

MCRT analysis of the isolated oils revealed a higher coking tendency for the liquefaction oils than for the pyrolysis oil. In fact, the cocking tendency of the oils appears to be related to their concentration of VR (Fig. 3). Hence, the content of VR needs to be minimized to avoid coking during subsequent upgrading to biofuel, e.g. using refinery processes, as proposed by van Rossum et al. [2].

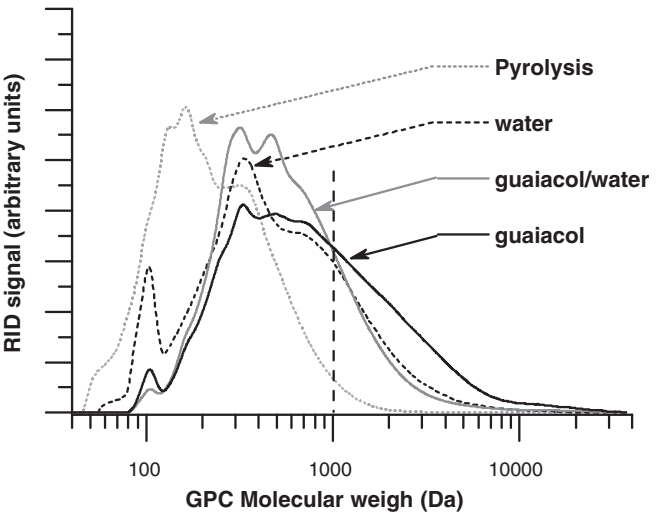

Fig. 2. GPC results of the isolated bio-oils.
Mw_{GPC} distribution of the isolated bio-oils; the small peak with Mw_{GPC} of 113 Da corresponds to a THF decomposition product. Liquefaction experiments performed at 300 °C during 30 min with 10 wt% of wood and 90 wt% of solvent (guaiacol, guaiacol/water and water). Pyrolysis experiment performed at 300 °C with residence times of 20–25 min for the solid particles and below 2 s for the oil.

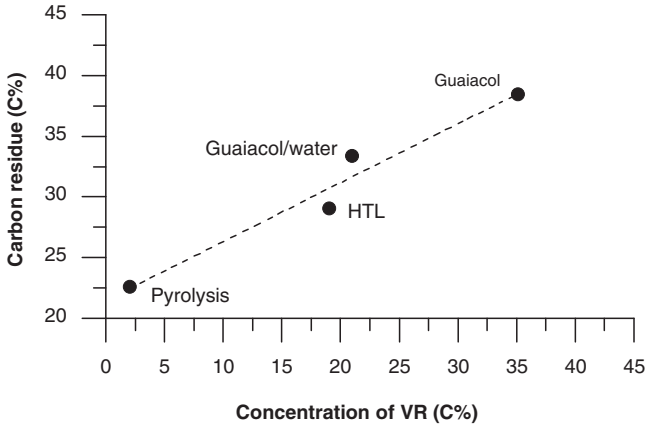

Fig. 3. MCRT results of the isolated bio-oils.
MCRT values represented versus the concentration of VR. Liquefaction experiments performed at 300 °C during 30 min with 10 wt% of wood and 90 wt% of solvent (guaiacol, guaiacol/water and water). Pyrolysis experiment performed at 300 °C with residence times of 20–25 min for the solid particles and below 2 s for the oil.

3.3.2. C:H:O analysis

The elemental analysis of the fractionated oils revealed a reduction in hydrogen and oxygen content in the bio-oils compared to the initial biomass. In fact, it showed a lignin-like composition for the GL and the GWL oils whereas it suggested a more dehydrated oil for WL and a less dehydrated oil for pyrolysis oil (Fig. 4). Between 35 and 45% of the oxygen present in wood is lost during liquefaction while only 20% of the oxygen is removed during pyrolysis. Larger deoxygenation during liquefaction in water, compared to pyrolysis, has already been reported in literature [26]. The combined H and O losses suggest significant dehydration of the biomass rather than decarboxylation to CO_2 (Fig. 4). Elimination of oxygen via formation of water is favored over CO_2 formation since dehydration is easier than decarboxylation, which requires a rearrangement of the carbohydrates to form carboxylic acids. Although counter-intuitive, an increase of water concentration in the reaction medium seems

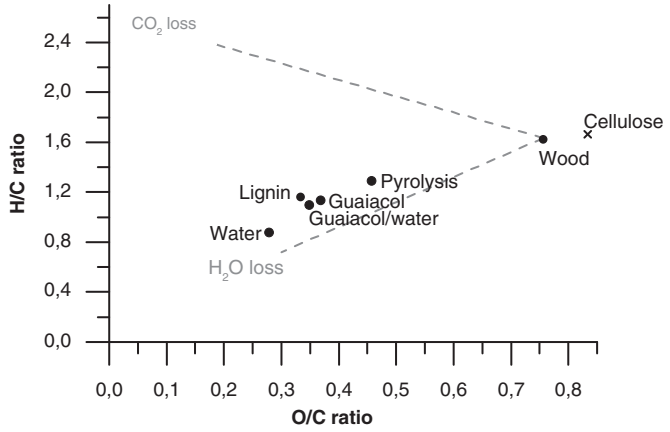

Fig. 4. Van Krevelen diagram of isolated bio-oils and model components.
Trend lines for wood dehydration and decarboxylation are also represented. Liquefaction experiments performed at 300 °C during 30 min with 10 wt% of wood and 90 wt% of solvent (guaiacol, guaiacol/water and water). Pyrolysis experiment performed at 300 °C with residence times of 20–25 min for the solid particles and below 2 s for the oil.

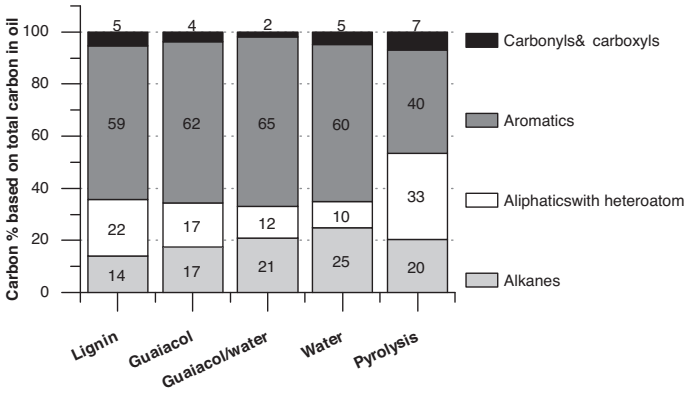

Fig. 5. ^{13}C NMR integration results of lignin and isolated bio-oils.
Integration regions for ^{13}C NMR assigned according to Section 2.6.3. Liquefaction experiments performed at 300 °C during 30 min with 10 wt% of wood and 90 wt% of solvent (guaiacol, guaiacol/water and water). Pyrolysis experiment performed at 300 °C with residence times of 20–25 min for the solid particles and below 2 s for the oil.

to promote the dehydration reactions (compared to GL, GWL has a 10% and WL a 40% more dehydration). This can be more clearly observed in the Van Krevelen diagram in Fig. C.3 (Supporting information) which combines the solids and the oils numerically. These results are consistent with the extensive dehydration reactions reported in the literature for hydrothermal liquefaction at elevated temperatures and pressures. For instance, degradation of cellulose and hemicellulose was reported to occur through a combination of dehydration and hydrolysis reactions [27].

3.3.3. ^{13}C and ^{1}H NMR analysis

The ^{13}C NMR spectra revealed similar chemical structures for all three liquefaction oils and for an organosolv lignin: approximately 60 C% of unsaturated aromatic carbons (105–166 ppm), 30 C% of saturated alkane-like (1–54 ppm) or carbohydrate-like carbons (54–105 ppm) and a minor percentage of unsaturated carbonyl and carboxyl carbons (166–210 ppm). In contrast, pyrolysis oil contained less aromatic carbons (40 C% vs. 60 C%) and a more carbohydrate-like carbon (33 C% vs. 10–22 C%, Fig. 5). The high carbohydrate-like carbon content is in accordance with the high oxygen content found in the pyrolysis bio-oil by the elemental

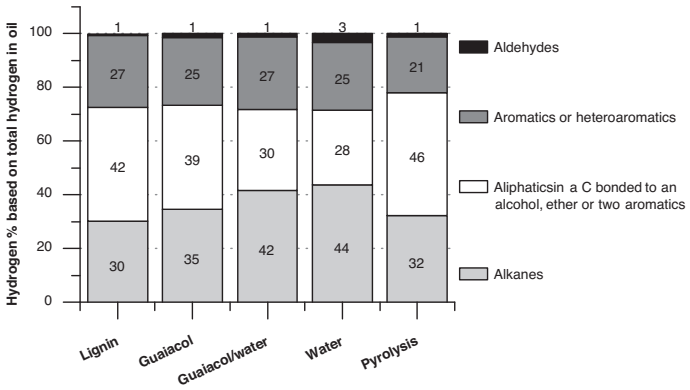

Fig. 6. ^{1}H NMR integration results of lignin and isolated bio-oils.
Integration regions for ^{1}H NMR assigned according to Section 2.6.4. Liquefaction experiments performed at 300 °C during 30 min with 10 wt% of wood and 90 wt% of solvent (guaiacol, guaiacol/water and water). Pyrolysis experiment performed at 300 °C with residence times of 20–25 min for the solid particles and below 2 s for the oil.

analysis (Fig. 4). Further details of the NMR analysis and results are presented in the supporting information.

For the three liquefaction experiments, 70–90 C% of the initial biomass is converted to an oil with a lignin-like composition. However, only a 40 C% of the initial biomass consists on lignin. Therefore, some of the carbohydrates present in the wood must have been converted to aromatics that are similar to those contained in lignin. Pyrolysis experiment leads to a bio-oil with lower yield and lower aromatic content than the liquefaction oils. Unfortunately it is not possible to determine if these aromatics have entirely lignin origin or if they are also partly carbohydrate derivatives. In addition, the completely opposite trends followed by the carbohydrate-like and alkane-like carbons suggest that the increase in water concentration in the liquefaction medium promotes the conversion of ether/hydroxyl groups to alkane groups. This shift suggests hydrogen transfer within the oil molecules to form alkane groups either from lignin [5,28,29] or from carbohydrates [30,31].

^{1}H NMR leads to the same conclusions as the ^{13}C NMR. The liquefaction oils show a content of aromatic hydrogen and carbohydrate-like hydrogen that resemble that of organosolv lignin but that contrasts with pyrolysis oil (with less aromatic hydrogen and more carbohydrate-like hydrogen than lignin and liquefaction oils, Fig. 6). The breakdown observed in ^{13}C and ^{1}H NMR is not expected to be quantitatively identical because of the varying H:C ratio expected for the various types of carbons.

3.3.4. FTIR analysis

The FTIR spectra of the middle fractions of bio-oils (Fig. 7) point to the same conclusions than the ^{13}C and the ^{1}H NMR. Liquefaction oils show mostly the vibration bands observed also for organosolv lignin: the typical aromatic peaks in the range 1400–1600 cm^{-1}, an unconjugated carbonyl or carboxyl peak at 1700 cm^{-1} and the C—H stretch from the aromatic molecules over 2900 cm^{-1}. The small concentration of carbohydrates in the liquefaction oils can be detected through the modest band just over 1000 cm^{-1} corresponding to the C—O stretching vibration and through the C—H stretch from aliphatic carbons under 2900 cm^{-1}. The three liquefaction bio-oils also present a broad and undefined band at 1200 cm^{-1}, which is best seen for the WL oil. This band has not been clearly assigned yet, but it is believed to belong to oxygenated aromatic compounds formed by fused phenols and furans based on evaluation of numerous aromatic components (see Appendix B) and literature data [15]. This agrees with their higher concentration of aromatic oxygenates compared to pyrolysis oil. In contrast, the pyrolysis oil shows weaker aromatic bands and stronger

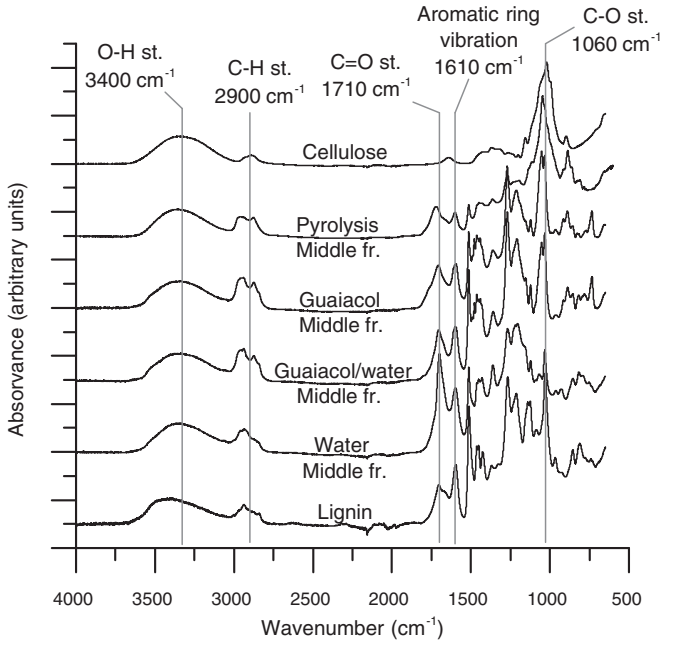

Fig. 7. Normalized FTIR spectra of model components and the middle fraction of the liquefaction and pyrolysis oils.
All the FTIR spectra of the fractions of the four oils can be found in the Supporting information. Liquefaction experiments performed at 300 °C during 30 min with 10 wt% of wood and 90 wt% of solvent (guaiacol, guaiacol/water and water). Pyrolysis experiment performed at 300 °C with residence times of 20–25 min for the solid particles and below 2 s for the oil.

carbohydrate bands, confirming the lower concentration in lignin-like compounds and the higher concentration of carbohydrate-like components compared to liquefaction oils. Besides, the WL oil presents the strongest carbonyl band (1710 cm^{-1}), suggesting a higher concentration of this functional group. However, this result does not completely match with the ^{13}C NMR results, in which similar concentrations of carbonyl and carboxyl groups are observed for the four oils.

3.4. Characterization of bio-oil fractions

As mentioned previously, liquefaction oils have a relatively high content of vacuum residue (VR), which causes several problems such a high coking tendency of these oils. Therefore, a characterization of the VR was performed to determine its composition. To this end, the heavy and the middle fractions (for GL and GWL) and, when convenient, the light fraction (WL and pyrolysis) were analyzed with GPC, EA, FTIR, ^{1}H NMR and ^{13}C NMR. The quality of the middle and heavy fractions of the GL bio-oil is illustrated in Figs. 8 and 9. Their corresponding average Mw_{GPC} are 360 Da and 1000 Da, respectively.

For GL, similar compositions were observed for the middle and the heavy oil fractions. The Elemental composition (Table C.2 in Supporting information) reveals that the heavy fraction has a lignin-like composition while the middle fraction has a slightly higher oxygen content (Fig. 8). Similarly, the NMR and The FTIR spectra show marginal differences between the two oil fractions (Tables C.4, and C.7 and Fig. C.6, Supporting information).

The middle and heavy fractions of the bio-oil obtained after GWL also present very similar composition and chemical structure, as observed from their elemental composition (Table C.2 in Supporting information), the ^{13}C and ^{1}H NMR (Tables C.4 and C.7, Supporting information), and the FTIR (Fig. C.6, Supporting information). Both fractions have a composition and structure very similar to lignin. The small differences observed in the elemental composition indicate a slightly larger dehydration in the middle fraction than in the heavy fraction. This matches the slightly higher concentration in aromatics and lower content in aliphatic components observed in the ^{13}C NMR and the ^{1}H NMR results.

As for the WL, the middle fraction and the heavy fraction had also practically the same composition and structure, as can be observed from their elemental composition (Table C.2 in Supporting information), the FTIR spectra (Fig. C.8, Supporting information) and the ^{13}C NMR (Table C4 and C.5, Supporting information). The lightest fraction is mainly composed of relatively small molecules that contain remarkably higher H/C ratio and lower O/C ratio than the two heavier fractions (see elemental composition in Table C.2, and GC–MS results in Table C.9 and Fig. C1, Supporting information).

The middle and heavy fractions obtained from pyrolysis oil contain a large concentration of both aromatics and carbohydrates, as measured by FTIR and ^{13}C NMR (Fig. C.10 and Table C.5, Supporting information). However, the heavy fraction has a higher concentration of aromatic and alkane compounds and a lower concentration of carbohydrates than the middle fraction, namely 48 C% of aromatics (vs. 40 C%) and 25 C% of alkanes (vs. 18 C%). The lightest fraction was mainly composed of small oxygenates (e.g. acetic acid, hydroxyacetone/propanal, furfural and various phenolic compounds) with higher H/C and O/C ratios than the two heavier fractions (see elemental composition in Table C.2 and GC–MS results in Table C.9 and Fig. C1, Supporting information).

4. Discussion

4.1. Process severity

In this study, severity of the reactions is used as a qualitative indication of the unconverted carbohydrates and residual oxygen content of both oil and solid residues. Increase in severity expresses decrease in unconverted carbohydrates and residual oxygen.

The combination of structure and yield of the solid indicates that the increase in water concentration in the reaction medium increases the reaction severity and therefore the reaction rates during liquefaction. Accordingly, a 19 C% of unconverted wood is obtained in GL, nearly no unconverted wood and no char is produced in the GWL (0.3 C%) and a 25 C% of char is obtained in WL.

The increase in process severity with the increase in water concentration is also apparent in the composition of the liquefaction oils. With the increase in water concentration, the extend in dehydration reactions increases, leading to oils with lower oxygen content. Also, the carbohydrates fingerprint in the FTIR and ^{13}C-spectra spectra disappears and the typical bands attributed to oxygenated aromatics become more significant. In conclusion, the severity of the reaction conditions, indicated by the amount of unconverted carbohydrates and oxygen content both in the oil and the solid residue, is: GL < GWL < WL.

Determining the severity of the pyrolysis is more complex than for liquefaction because oil and char have different residence time in the hot reaction zone. For instance, residence time is lower than 2 s for the oils, but between 20 and 25 min for the char. Accordingly, the oil seems to have been produced at moderate severity, as indicated by its high oxygen and carbohydrate content.

4.2. Chemistry of liquefaction

After isolation and fractionation, the chemical composition and structure of the bio-oils and their fractions were analyzed. The characterization results revealed that, during wood liquefaction, aromatic and alkane-like carbon is formed. The origin of this type of carbon as well as the possible reaction mechanisms for their formation are discussed below.

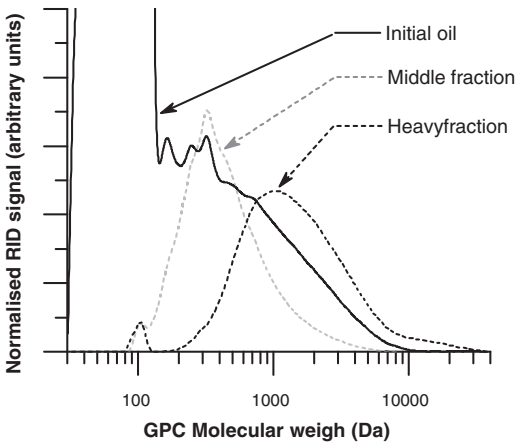

Fig. 8. GPC of GL bio-oil fractions.
Mw distribution of the middle and heavy fraction of bio-oil obtained in guaiacol (GL) (The small peak with MwGPC of 113 Da corresponds to a THF decomposition product. GL performed at 300 °C during 30 min with 10 wt% of wood and 90 wt% of guaiacol).

NMR and FTIR analyzes of the liquefaction oils reveal a yield of aromatics (40–60C%, see Appendix C) that is higher than the aromatics available in the lignin of untreated wood (25 C%, see appendix C). This suggests that carbohydrates are converted to aromatic products, and agrees with the dehydration of the initial biomass observed in the Van Krevelen diagrams of the oils (Fig. 4). Unfortunately, the aromatic content in the pyrolysis oil is similar to the aromatic content in the initial biomass, so it cannot be determined whether these aromatics have lignin or carbohydrate origin. The limited formation of CO_2 can be attributed to the decarboxylation of organic acids such as levulinic or lactic acid, typically formed during thermal treatment of carbohydrates [32,33].

The conversion of carbohydrates to aromatic compounds such as furans and phenols during liquefaction and pyrolysis has been largely reported in literature, and numerous reaction mechanisms have been proposed [34–37]. According to most publications, the degradation of a carbohydrate polymer, for example cellulose, generally proceeds via a first depolymerisation to form oligomers and monomers (glucose in this case). At those conditions, glucose is relatively unstable and undergoes fast degradation reactions such as dehydration (to form anhydro-sugars), isomerisation (generally to form fructose), or retro-aldol reactions (to form light oxygenated

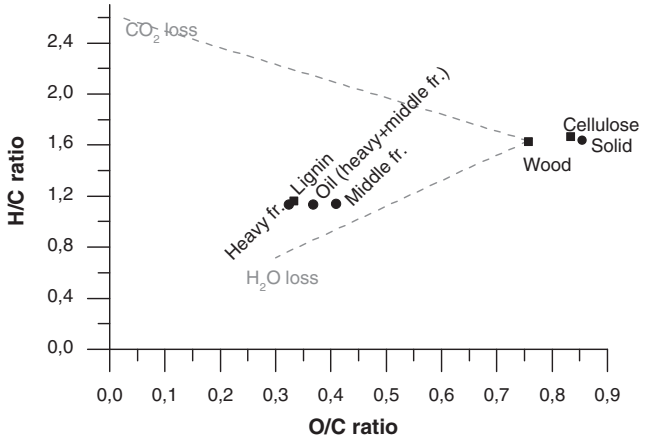

Fig. 9. Van Krevelen diagram of GL bio-oil fractions.
Atomic composition of the middle and heavy fraction of bio-oil obtained in guaiacol (GL) (GL performed at 300 °C during 30 min with 10 wt% of wood and 90 wt% of guaiacol).

compounds such as glycolaldehyde or dihydroxyacetone). Glucose can also be converted to furanic compounds through the dehydration of fructose or anydro-sugars [34]. Some publications, however, report the formation of furans directly from cellulose and also the direct dehydration of cellulose to form furanic polymers [34,35]. Likewise, the formation of benzene or phenolic structures from carbohydrates has also been reported [36–38]. Luijkx et al. [36], for example, observed the formation of 1,2,4-benzenetriol during the hydrothermal liquefaction of 5-(hydroxymethyl)-2-furaldehyde (HMF) and D-fructose. Cheng et al. [38] studied the reaction of furans with olefins over a zeolite catalyst via Diels-Alder condensations, which lead to the formation of aromatics with benzene rings. The same type of reaction can be expected between two furanic molecules to form benzene rings. Pastorova et al. [37] characterized the char formed from microcrystalline cellulose and identified several furans with aliphatic side chains and a range of benzene and phenol derivatives. Furthermore, they observed that the aromatic intermediates formed during the thermal treatment condensed with other aromatics or small reactive molecules to form char. Hence, furanic and phenolic compounds can be formed from the thermal treatment of carbohydrates, indicating that the aromatics present in bio-oils do not necessarily have lignin origin. Unfortunately, none of available analyzing techniques could differentiate between furanic and phenolic compounds. This question will be addressed in more depth in a future paper that investigates the liquefaction of pure carbohydrates and lignin.

The concentration of alkane-like carbon (aliphatic carbon without oxygen substituents) in the bio-oils is shown to increase with increasing process severity, which indicates that these type of functionalities are formed during the liquefaction and pyrolysis of the biomass. Lignin has been reported to partly decompose to aliphatic functionalities. For instance, Ben et al. [5] and Barbier et al. [28] observed their formation during the pyrolysis of softwood kraft lignin and during the hydrothermal conversion of alkali lignin and model compounds. Formation of alkane-like carbon was also observed by Britt et al. [29] when they performed flash vacuum pyrolysis (FVP) of methoxy-substituted β—O—4 lignin model compounds. They observed that the main reactions taking place during the thermal treatment of lignin were the fragmentation of the ether bonds and the alkylation of the aromatic rings of the intermediate products. As a result of these reactions, new aliphatic C_{aliph}—C_{arom} bonds were formed. Alkane-like components could also be formed from carbohydrates via hydrogen transfer (intermolecular) or hydrogen shift (intramolecular). For example, Girisuta et al. studied the conversion of glucose to levulinic acid (with three alkane-like carbons) with HMF as a reaction intermediate [30], and Antal et al. observed the formation of lactic acid (with one alkane-like carbon) from dihydroxyacetone and glyceraldehyde [31].

Only minor differences in chemical structure are observed between the various fractions of bio-oils. Heavy fractions tend to contain slightly more aromatic components than the lighter fractions, which are usually richer in aliphatic compounds. The resemblance between the various fractions of a bio-oil suggests that they are formed via the same type of reactions.

A future paper will report on the liquefaction of wood model components (cellulose, hemicellulose and lignin) to deepen the understanding of the chemistry of liquefaction.

4.3. Oil quality

Liquefaction appears to remove more oxygen than pyrolysis does (35–45 wt% vs. 20 wt%) and the deoxygenation appears to decrease in the order of WL > GWL > GL > Pyrolysis. In all cases, dehydration is the dominant mechanism for oxygen elimination and, consequently, all the oils have a similar effective

Table 2
HHV of bio-oils, model components and fossil fuels.

Experiment	HHV (MJ/kg)
GL bio-oil	25.7
GWL bio-oil	26.1
WL bio-oil	27.2
Pyrolysis bio-oil	23.8
Cellulose	17.4
Lignin	27.0
Wood	18.6
Diesel	46
Gasoline	44.8–46.9

hydrogen/carbon ratio of H/C_{eff} = 0.32–0.40 (Table C.2 supporting information). The equation used to calculate the H/C_{eff} ratio is shown in Section 5. As a result of the oxygen content and the hydrogen/carbon effective ratio, the various liquefaction bio-oils are estimated to have approximately 50% higher heating value (HHV) than the wood and approximately 10% higher than pyrolysis oil (see Table 2). However, the values are still modest compared to typical transportation fuels such as diesel or gasoline. The HHVs were calculated using the Reed's formula [18] (Section 2.5, product definition and calculation). HHV of diesel and gasoline obtained from [39].

As observed from their composition, the four bio-oils need to be upgraded before being used as transport fuels. Upgrading requires deeper deoxygenation as well as deeper cracking or depolymerisation. Such upgrading has been proven in the case of pyrolysis oil, where the oil was subjected to a partial hydrotreatment and, subsequently, to catalytic cracking by co-feeding in an FFC unit [40]. A similar strategy can be adopted for the liquefaction oils with minor modifications for they offer the advantage of lower O content but the penalty of higher Mw_{GPC} and, consequently, higher coking tendency.

4.4. Fractionation methodology

A procedure for bio-oil fractionation with GPC was developed, allowing the separation of bio-oil from the liquefaction solvent as well as the partition of these bio-oil into several fractions based on molecular $weight_{GPC}$. The use of GPC fractionation allowed an important decrease in the error of the analyzes performed (EA, FTIR and MCRT). Furthermore, ^{13}C NMR analysis of the bio-oil would have been impossible without fractionation because of the dominant signature of the liquefaction solvent. The details are reported in the supporting information. Nevertheless, further improvements of the fractionation technique should be considered.

In some cases, namely WL and pyrolysis oils, a fraction of the bio-oil (Mw_{GPC}~300–1000 Da) was lost during the fractionation, most likely due to poor dissolution and sticking vessel walls (see supporting information). This problem can probably be solved by choosing an adequate eluent that completely dissolves these oils. Important requirements for this eluent are its compatibility with the column packing, having a low boiling point (to be easily removed after fractionation), not promoting specific chemical interaction of the bio-oil with the column packing that could disturb size-based separation and low response in the RI and UV detectors.

Furthermore, better separation of bio-oil fractions can be obtained by adding more columns into the system or by varying the column packing or the mobile phase.

5. Conclusions

Three liquefaction oils and one fast pyrolysis oil were prepared, analyzed and compared. Liquefaction oils were prepared by heating 10 wt% of pine wood during 30 min at 300 °C in guaiacol, a guaiacol and water mixture and in water. Pyrolysis oil was obtained treating pine wood at 500 °C with residence times of 20–25 min for the solid particles and below 2 s for the oil. To be able to characterize the liquefaction oils, they were first isolated from the liquefaction solvent using Gel Permeation Chromatography (GPC) preparative fractionation. This technique also enabled the fractionation of the oils into several fractions based on apparent molecular weight, allowing to study the change in composition and oil properties with the molecular weight.

The characterization of the four bio-oils showed major differences between pyrolysis and liquefaction oils. Compared to the pyrolysis oil, the three liquefaction oils showed a lower oxygen content and, correspondingly, a higher heating value. Based on NMR and FTIR, the liquefaction oils resemble lignin and contain more aromatic (phenolic/furanic) functionalities and less carbohydrate-like functionalities than pyrolysis oil. However, they also show a much heavier tail, with approximately 1/3 of the bio-oil having an apparent Mw_{GPC} beyond 1000 Da. As a result, the liquefaction oils have a much higher coking tendency. Interestingly, the heaviest fraction did not differ significantly from the lightest one in terms of atomic composition and chemical functionalities.

The high yield of lignin-like aromatic carbon in the oils, compared to the aromatic content of the unreacted wood, indicates that carbohydrates have to contribute to the formation of these lignin-type of compounds. Besides, alkane-like carbon is also produced, which could have either or both lignin and carbohydrate origin.

Dehydration was found to be the main deoxygenation mechanism in the four processes and, within liquefaction oils, the extend on dehydration increased when increasing the water concentration in the reaction medium.

Based on the amount unconverted carbohydrates and oxygen content both in the oil and the solid residue, a ranking of the severity of the liquefaction reaction conditions, is proposed: Guaiacol < Guaiacol/water < Water. This indicates that the severity increases with increasing concentration of water in the liquefaction medium. As for Pyrolysis, the oil indicates a mild severity while the char indicate a high severity, which can be explained by their respectively short and long residence time.

The quality of the bio-oils was improved compared to the initial biomass (in terms of oxygen content, H/C effective ratio and Higher Heating Value), but it is still quite distant from the typically used transport fuels.

Acknowledgements

The authors would like to thank Shell Global Solutions International B.V. for funding this research, and Benno Knaken, Erna Fränzel-Luiten and Bianca Snellink-Ruël for the technical support.

Appendix A. Supplementary data

Supplementary data associated with this article can be found, in the online version, at http://dx.doi.org/10.1016/j.jaap.2015.03.005.

References

[1] Shell Scenarios Team, Shell Energy Scenarios to 2050: Signals & Signposts (2011).
[2] G. van Rossum, W. Zhao, M. Castellvi Barnes, J.-P. Lange, S.R.A. Kersten, ChemSusChem 7 (2014) 253.
[3] H. Ben, A.J. Ragauskas, ChemSusChem 5 (2012) 1687.
[4] M.E. Boucher, A. Chaala, H. Pakdel, C. Roy, Biomass Bioenergy 19 (2000) 351.
[5] H. Ben, A.J. Ragauskas, Energy Fuels 25 (2011) 2322.
[6] M. Garcia-Perez, A. Chaala, H. Pakdel, D. Kretschmer, C. Roy, Biomass Bioenergy 31 (2007) 222.
[7] R. Fahmi, A.V. Bridgwater, I. Donnison, N. Yates, J.M. Jones, Fuel 87 (2008) 1230.
[8] B. Scholze, C. Hanser, D. Meier, J. Anal. Appl. Pyrolysis 58–59 (2001) 387.

[9] Y.-H.E. Sheu, C.V. Philip, R.G. Anthony, E.J. Soltes, J. Chromatogr. Sci. 22 (1984) 497.
[10] T. Andersson, T. Hyötyläinen, M.-L. Riekkola, J. Chromatogr. A 896 (2000) 343.
[11] D.G. Richards, C.E. Snape, K.D. Bartle, C. Gibson, M.J. Mulligan, N. Taylor, Fuel 62 (1983) 724.
[12] D.L. Wooton, W.M. Coleman, L.T. Taylor, H.C. Dorn, Fuel 57 (1978) 17.
[13] C.W. Curtis, C.D. Hathaway, J.A. Guin, A.R. Tarrer, Fuel 59 (1980) 575.
[14] W.J.J. Huijgen, A.T. Smit, P.J. de Wild, H. den Uil, Bioresour. Technol. 114 (2012) 389.
[15] S. Kumar, J.-P. Lange, G. Van Rossum, S.R.A. Kersten, Ind. Eng. Chem. Res. 53 (2014) 11668.
[16] R.J.M. Westerhof, D.W.F. Brilman, M. Garcia-Perez, Z. Wang, S.R.G. Oudenhoven, W.P.M. van Swaaij, S.R.A. Kersten, Energy Fuels 25 (2011) 1817.
[17] M. Ahmad, A.U. Rajapaksha, J.E. Lim, M. Zhang, N. Bolan, D. Mohan, M. Vithanage, S.S. Lee, Y.S. Ok, Chemosphere 99 (2014) 19.
[18] E.S. Domalski, T.L. Jobe, T.A. Milne, Thermodynamic data for biomass conversion and waste incineration, in: Solar Technical Information Program, National Bureau of Standards, Washington, 1986.
[19] L. Ingram, D. Mohan, M. Bricka, P. Steele, D. Strobel, D. Crocker, B. Mitchell, J. Mohammad, K. Cantrell, C.U. Pittman, Energy Fuels 22 (2007) 614.
[20] C.A. Mullen, G.D. Strahan, A.A. Boateng, Energy Fuels 23 (2009) 2707.
[21] S. Kersten, M. Garcia-Perez, Curr. Opin. Biotechnol. 24 (2013) 414.
[22] Z. Wang, B. Pecha, R.J.M. Westerhof, S.R.A. Kersten, C.-Z. Li, A.G. McDonald, M. Garcia-Perez, Ind. Eng. Chem. Res. 53 (2014) 2940.
[23] J. Akhtar, N.A.S. Amin, Renew. Sustain. Energy Rev. 15 (2011) 1615.
[24] D. Mohan, C.U. Pittman, P.H. Steele, Energy Fuels 20 (2006) 848.
[25] D. Knežević, Hydrothermal conversion of biomass, University of Twente, The Netherlands, 2009, pp. 151, PhD Dissertation.
[26] D.C. Elliott, G.F. Schiefelbein, Liquid hydrocarbon fuels from biomass, American Chemical Society, Division of Fuel Chemistry Annual Meeting Preprints vol. 34 (1989) 1160–1166.
[27] A.A. Peterson, F. Vogel, R.P. Lachance, M. Fröling, J.M.J. Antal, J.W. Tester, Energy Environ. Sci. 1 (2008) 32.
[28] J. Barbier, N. Charon, N. Dupassieux, A. Loppinet-Serani, L. Mahé, J. Ponthus, M. Courtiade, A. Ducrozet, A.-A. Quoineaud, F. Cansell, Biomass Bioenergy 46 (2012) 479.
[29] P.F. Britt, A.C. Buchanan, M.J. Cooney, D.R. Martineau, J. Org. Chem. 65 (2000) 1376.
[30] B. Girisuta, L.P.B.M. Janssen, H.J. Heeres, Chem. Eng. Res. Des. 84 (2006) 339.
[31] M.J. Antal Jr., W.S.L. Mok, G.N. Richards, Carbohydr. Res. 199 (1990) 111.
[32] F. Shafizadeh, Y.Z. Lai, J. Org. Chem. 37 (1972) 278.
[33] H. Yang, R. Yan, H. Chen, D.H. Lee, C. Zheng, Fuel 86 (2007) 1781.
[34] F.-X. Collard, J. Blin, Renew. Sustain. Energy Rev. 38 (2014) 594.
[35] M.S. Mettler, S.H. Mushrif, A.D. Paulsen, A.D. Javadekar, D.G. Vlachos, P.J. Dauenhauer, Energy Environ. Sci. 5 (2012) 5414.
[36] G.C.A. Luijkx, F. van Rantwijk, H. van Bekkum, Carbohydr. Res. 242 (1993) 131.
[37] I. Pastorova, R.E. Botto, P.W. Arisz, J.J. Boon, Carbohydr. Res. 262 (1994) 27.
[38] Y.-T. Cheng, G.W. Huber, Green Chem. 14 (2012) 3114.
[39] Kaye and Laby, Tables of Physical and Chemical Constants, National Physical Laboratory, 2014, http://www.kayelaby.npl.co.uk/.
[40] F. de Miguel Mercader, M.J. Groeneveld, S.R.A. Kersten, N.W.J. Way, C.J. Schaverien, J.A. Hogendoorn, Appl. Catal. B Environ. 96 (2010) 57.